sustainability

MDPI

Article

A Bi-Band Binary Mask Based Land-Use Change Detection Using Landsat 8 OLI Imagery

Xian Li [1,2], Shuhe Zhao [1,2,3,*], Hong Yang [4,5,*], Dianmin Cong [1,2] and Zhaohua Zhang [1,2]

1 School of Geographic and Oceanographic Sciences, Nanjing University, 163 Xianlin Ave, Qixia District, Nanjing 210023, China; sureli93@outlook.com (X.L.); njucdm_job@163.com (D.C.); zhangzhaohua0730@163.com (Z.Z.)
2 Jiangsu Provincial Key Laboratory of Geographic Information Science and Technology, Nanjing University, 163 Xianlin Ave, Qixia District, Nanjing 210023, China
3 Jiangsu Center for Collaborative Innovation in Geographical Information Resource Development and Application, Nanjing 210023, China
4 Norwegian Institute of Bioeconomy Research (NIBIO), Postboks 115, 1431 Ås, Norway
5 CEES, Department of Biosciences, University of Oslo, Blindern, 0316 Oslo, Norway
* Correspondence: zhaosh@nju.edu.cn (S.Z.); hongyanghy@gmail.com (H.Y.); Tel.: +86-25-8968-1015 (S.Z.); +47-9699-1156 (H.Y.)

Academic Editor: Marc A. Rosen
Received: 5 January 2017; Accepted: 17 March 2017; Published: 22 March 2017

Abstract: Land use and cover change (LUCC) is important for the global biogeochemical cycle and ecosystem. This paper introduced a change detection method based on a bi-band binary mask and an improved fuzzy c-means algorithm to research the LUCC. First, the bi-band binary mask approach with the core concept being the correlation coefficients between bands from different images are used to locate target areas with a likelihood of having changed areas. Second, the improved fuzzy c-means (FCM) algorithm was used to execute classification on the target areas. This improved algorithm used distances to the Voronoi cell of the cluster instead of the Euclidean distance to the cluster center in the calculation of membership, and some other improvements were also used to decrease the loops and save time. Third, the post classification comparison was executed to get more accurate change information. As references, change detection using univariate band binary mask and NDVI binary mask were executed. The change detection methods were applied to Landsat 8 OLI images acquired in 2013 and 2015 to map LUCC in Chengwu, north China. The accuracy assessment was executed on classification results and change detection results. The overall accuracy of classification results of the improved FCM is 95.70% and the standard FCM is 84.40%. The average accuracy of change detection results using bi-band mask is 88.92%, using NDVI mask is 81.95%, and using univariate band binary mask is 56.01%. The result of the bi-band mask change detection shows that the change from farmland to built land is the main change type in the study area: total area is 9.03 km^2. The developed method in the current study can be an effective approach to evaluate the LUCC and the results helpful for the land policy makers.

Keywords: change detection; correlation coefficient; binary mask; Voronoi distance; fuzzy c-means; Landsat 8 OLI

1. Introduction

Land use and cover changes (LUCC) in earth's surface alter biogeochemical and hydrological cycles, and affect climate change and ecological balance [1]. Therefore, global and regional assessments on LUCC are important for climate and ecosystem [2]. It is of great importance to monitor the LUCC, for example in China where significant LUCC has happened in the last decades [3–6]. Change detection technology for remote sensing image has been applied in many areas such as land cover/land

use change detection [7,8], agricultural survey [9,10], urban sprawl monitoring [11,12], forest and vegetation monitoring [13,14], wetland monitoring [15,16], water quality monitoring [17,18], disaster evaluation [19,20] and so on [21].

Many change detection techniques have been developed, for example, post-classification comparison (PCC), image differencing, principle components analysis, and vegetation index differencing and so on [22,23]. Singh [24] grouped the change detection technique into two categories, comparative analysis of independently produced classifications for different dates and simultaneous analysis of multi-temporal data, according to the classification of image and the sequence of comparison for the bi-temporal images. Lu [25] figured out that the image differences is the most widely used method for change detection in algebra change detection methods. Bovolo et al. [26] used Landsat TM5 from two temporal images to produce the multi-spectral difference images, and then used Support Vector Domain Description (SVDD) to classify and produce the change detection maps. Ghosh and others [27–29] used Landsat TM7 and Landsat TM5 images to produce the difference images, and then hybridized the fuzzy c-means and Gustafson–Kessel clustering with two optimization techniques (genetic algorithm and simulated annealing) to classify the images. Zanotta and Haertel [30] transformed images from two temporal ones to fraction images, used the fraction images to calculate difference image, defined change in terms of degrees of membership to the class "change", and produced the fuzzy change maps. Chen and Cao [31] identified edges in different images produced from bi-temporal images, and applied Markov random field based approaches to adjust the threshold to realize the change detection. As another most used change detection, PCC plays an important role in change detection researches. The classification step in PCC greatly influences the final accuracy of the change detection results [32]. Unsupervised classification, because avoids the manual intervention, decreases the influence of the subjective factor of researchers and does not need training data, is often chosen to execute the classification [33]. Shalaby and Tateishi [34] applied the maximum likelihood classification method on the bi-temporal images, and post-classification change detection technique was applied successfully. The maximum likelihood classification method has been applied on the bi-temporal images, and obtained the change information via post-classification comparison [35,36].

Hussain et al. [22] suggested that the image differencing approach is relatively simple and easy to interpret results. The post-classification comparison can reduce the influences from atmospheric, sensor and local disturbance; minimize the effects of using multi-sensor images and produce the complete matrices of change. However, there are drawbacks of these two change detection methods. The image difference approach does not have complete matrices of change information and it is difficult to select the optimal threshold; the same value may have different meanings depending on the starting class [22]; and too much information would be discarded in the subtraction process [24]. Regarding the PCC method, the final accuracy depends on classification accuracy of individual images, which can cause the accumulation of errors [22,32].

To minimize the limitations of image difference approach and improve the classification accuracy, this paper introduced a framework for change detection, which is the combination of a bi-band binary mask approach and an improved fuzzy c-means algorithm (FCM). It can make the most of information about the changed and unchanged areas to produce the complete change matrices. The bi-band binary mask approach takes account of the correlation coefficients of all corresponding bands in each image, and then uses the coefficients to choose proper bands to calculate the difference images, which helps to quickly identify the changed area. Finally, the improved FCM algorithm and post classification comparison were applied to distinguish which class the pixel belongs to and produce the complete matrix of changes. To evaluate the classification accuracy, both the improved FCM algorithm and the standard FCM algorithm were applied on images. The bi-band binary mask was used to locate a suspected changed area to be our target area, reducing the amount of processing data and execution time, especially in the pixel-based unsupervised classification algorithm. Regarding the capability of the bi-band binary mask, binary mask of the univariate and Normalized Difference Vegetation Indices (NDVI) difference images were used to execute the same change detection procedure, and the results

were compared. The combination of bi-band binary mask and fuzzy c-means algorithm for land-use change detection method was applied in Chengwu County, north China.

2. Materials and Methods

2.1. Study Area

Chengwu County is located in the southwest of Shandong Province, north China (Figure 1). Chengwu covers an area of 988.3 km^2 and is found within 115°43′57.6″E–116°10′07.5″E, and 34°48′21.8″N–35°09′44.0″N. Chengwu is located in an alluvial plain of the Yellow River, thus has flat topography. The average altitude is 45.5 m above sea level. The climate is a typical temperate climate: four distinct seasons, sufficient rainfall, and hot in summer. Agriculture is the primary industry of Chengwu.

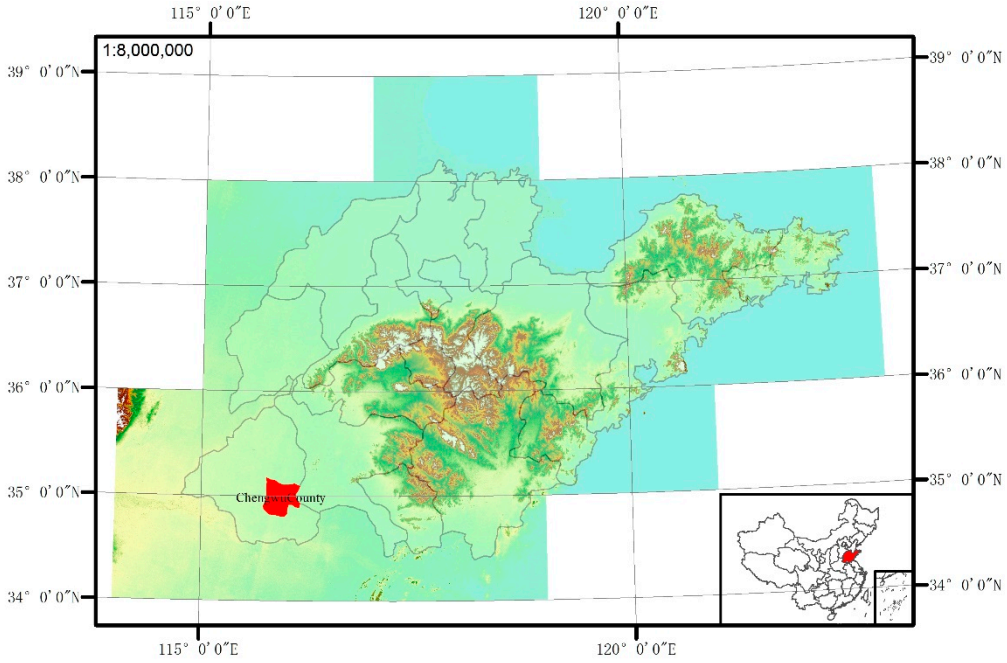

Figure 1. Location of the study area in China.

2.2. Dataset and Preprocessing

To evaluate the performance of the proposed method, two Landsat 8 OLI datasets were obtained from the U.S. Geological Survey (http://glovis.usgs.gov/). A pair of near-anniversary images was selected to minimize the error introduced by mere seasonal differences [37]. One dataset is from 22 August 2015, and the other is from 1 September 2013 (WGS 84, UTM, Zone 50N, path 123, row 034), with a pixel size of 30 m × 30 m for the spectral bands used (Figure 2). These images were selected based on the acquisition time, availability and quality of the datasets for the study area.

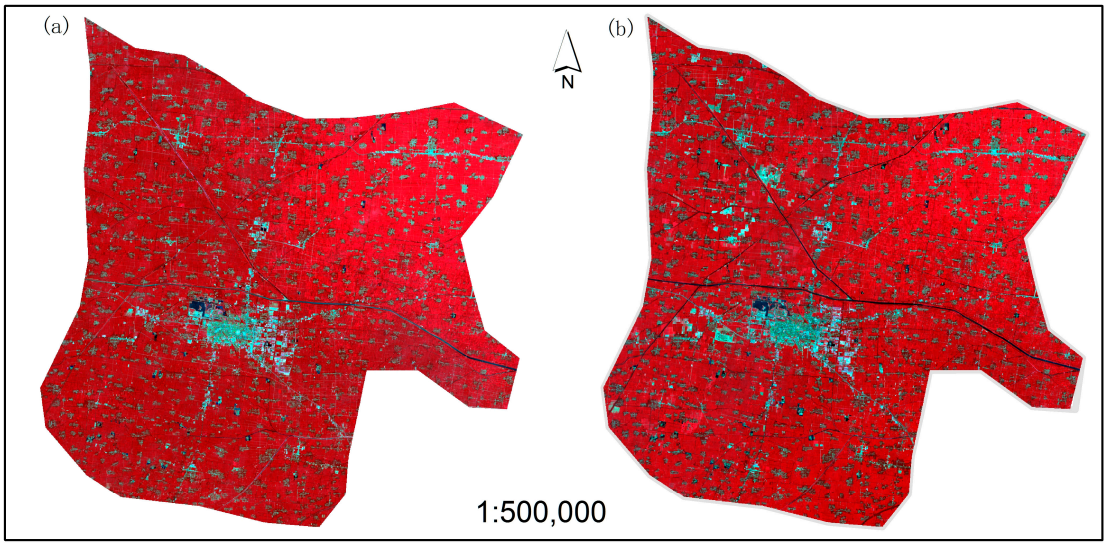

Figure 2. Landsat 8 OLI images of Chengwu County: (**a**) image in 2013; and (**b**) image in 2015.

The images were ortho-rectified and all of the multi-spectral bands were used to aid in the classification of images via the improved fuzzy c-means algorithm. Through the use of ENVI 5.1 (EXELIS VIS, Boulder, CO, USA), the radiometric calibration and FLAASH atmospheric correction were executed on the images, a histogram matching approach was executed on them to reduce differences caused by light condition and so on, which led to the difference in hue. The study area was subset via a shape file of Chengwu County.

2.3. Methods

This study introduces a change detection method based on a bi-band binary mask approach and an improved fuzzy c-means algorithm (FCM).

There are two important steps of this change detection method. One is the binary masks, which were used to mask off unchanged areas in the bi-temporal images, and a rough location of areas with a likelihood of change were remained and considered to be the target areas; the other is the improved FCM based unsupervised classification, which was executed on target areas in the two images to help to precisely locate changed areas in PCC.

There are several steps of this proposed change detection method (Figure 3). First, the binary mask was created and used to mask off unchanged areas in the two images. Second, the unsupervised classification method was executed on the changed areas on the two images. Third, the Post-Classification Comparison (PCC) method was applied to get the precise location of changed area and determine the change pattern. Fourth, the accuracy of the change detection results was evaluated before the final change map was determined.

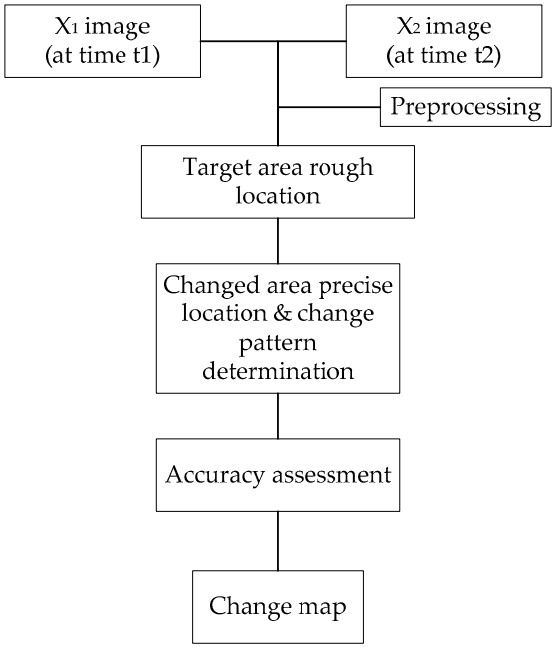

Figure 3. The flowchart of this study.

2.3.1. Target Area Rough Location

Target area rough location was realized through the use of a bi-band binary mask. The binary mask is derived from the bi-temporal images datasets according to the correlation parameter of each pair of corresponding bands. The binary mask was used to mask out areas with a likelihood of having changed. The detailed process is illustrated as Figure 4.

The correlation parameter is based on the observation that pairs of brightness values from the same geographic area between bi-temporal image datasets tend to be highly correlated when little change occurs, but they could be uncorrelated when big change occurs [38].

Corresponding bands refer to bands from two temporal images that share the same number of bands, e.g., band 1 from image 1 and band 1 from image 2 constitute a pair of corresponding bands. The correlation coefficients of each pair of corresponding bands were computed; the maximum of correlation coefficients indicates that this pair of bands contains more information about unchanged area than that of changed one, while the minimum indicates that this pair of bands contains more information about changed area. The pair(s) of bands that correspond to the minimum and the maximum value (B_{min1} and B_{min2}, and B_{max1} and B_{max2}) were selected to create difference images (D_{min} and D_{max}), separately. Then, thresholds were selected to separate the changed areas from unchanged areas for the difference images. The changed areas were labeled as 1 and the unchanged areas were labeled as 0. The two binary mask datasets were created: one for the least correlated bands (CA_1) and the other for the most correlated bands (CA_2). The next step is to combine these two binary mask datasets using the logistic operator OR. The combined binary mask data were used to roughly locate the changed areas quickly.

To evaluate the validity of this bi-band binary mask, two other binary masks (the NDVI difference binary mask and the univariate image difference binary mask) were created to compare.

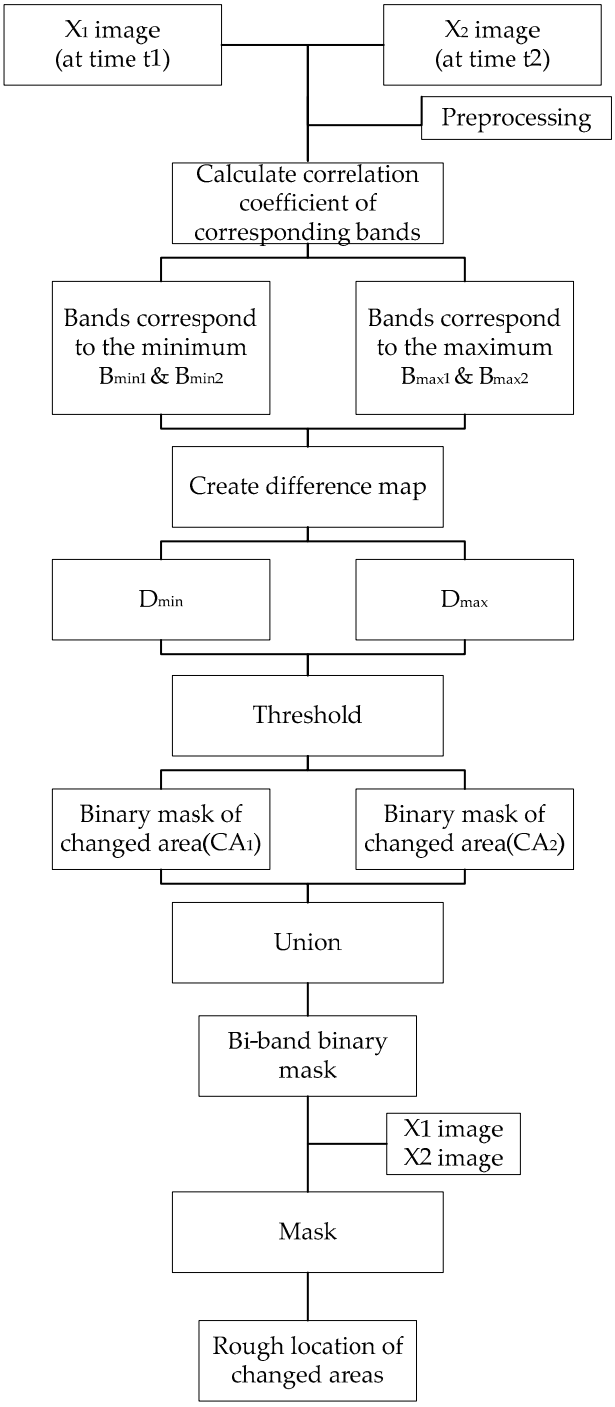

Figure 4. Target area rough location.

2.3.2. The NDVI Difference Binary Mask and Univariate Image Difference Binary Mask

Vegetation change detection is an important content for change detection. NDVI is sensitive for the vegetation change, and the NDVI differencing has been widely used for vegetation monitoring [35,36]. Considering the high vegetation coverage of the study area, the NDVI difference binary mask was selected due to its sensitivity to vegetation change. Due to its simple and intuitive theory, the univariate image differencing is the most widely applied change detection algorithm [33,34], and the univariate image difference binary mask was also selected for comparison.

The NDVI binary mask was the result of NDVI difference threshold segmentation. The NDVI difference was calculated through the NDVI subtraction between the two images. The univariate image differencing binary mask was the result of singe band difference threshold segmentation. Fan et al. [39] found that when choosing single band data to calculate difference images, band 2 (0.52–0.60 μm) data in Landsat TM image should be the first priority considering the physical characteristics. Band 2 in Landsat TM image corresponds to band 3 (0.53–0.59 μm) in Landsat 8 OLI image. Therefore, band 3 image data of the study area were chosen to calculate the univariate difference image.

Thresholds for these two difference images were determined by trial and error.

2.3.3. Changed Area Precise Location and Change Pattern Determination

For the precise location of change area, here an improved fuzzy c-means algorithm was used to eliminate false areas in the rough location of changed area. A post classification comparison was executed to determine the change pattern. The flow chart is illustrated as Figure 5.

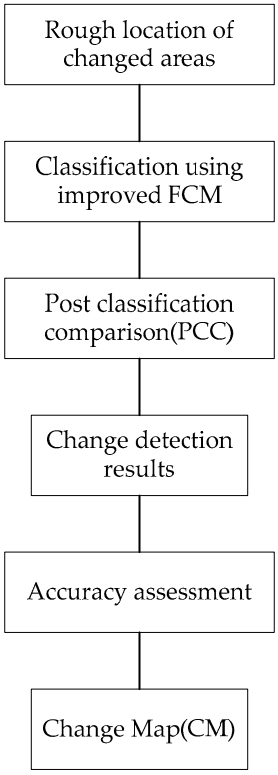

Figure 5. Changed area precise location and change pattern determination.

To know the concrete From–To information of the changed areas, classifications were executed on the bi-temporal image datasets. Here, an improved fuzzy c-means algorithm (FCM) was used to execute an unsupervised classification. This algorithm combined the improvements put forward by Höppner et al. [40], Kolen et al. [41] and Yang et al. [42]. Höppner et al. [40] found that some properties of the membership functions defined in the standard fuzzy c-means are undesirable at least in some application areas, for example the small peaks of high membership degrees are supposed to be avoided and the membership degrees are supposed to be crisper. To solve these problems, they used distances to the Voronoi cell of the cluster instead of the Euclidean distance to the cluster center during membership calculation, and the result was found to be more effective, and much closer to those of the crisp original methods. It was also less sensitive to noise and outliers. Zhu et al. [43] also proved the feasibility of this improved FCM algorithm in their study. In mathematics, a Voronoi diagram is a partitioning of a plane into regions based on distance to points in a specific subset of the plane.

That set of points (called seeds, sites, or generators) is specified beforehand, and for each seed there is a corresponding region consisting of all points closer to that seed than to any other. These regions are called Voronoi cells. The Voronoi diagram of a set of points is dual to its Delaunay triangulation (https://en.wikipedia.org/wiki/Voronoi_diagram).

The formulas involved in this improved fuzzy c-means algorithm are as follows:

$$u_{i,j} = \frac{1}{\sum_k^c \left(\frac{d_V(x_j, p_i)}{d_V(x_j, p_k)} \right)^{\frac{1}{m-1}}} \tag{1}$$

$$p_i = \frac{\sum_{j=1}^n u_{i,j}^m x_j}{\sum_{j=1}^n u_{i,j}^m} \tag{2}$$

where $x_j \in X$, $j \in \{1, \ldots, n\}$ means the datum, $p_i \in P$, $i \in \{1, \ldots, c\}$ means the cluster, d_E means the Euclidean distance, d_V means the Euclidean distance to the border of Voronoi cell, and $u_{i,j}$ means the membership degree.

$$d_V(x, p_i) = \frac{1}{2}(d_E^2(x, p_i) - \min_{1 \le s \le c} d_E^2(x, p_s)) \tag{3}$$

Noteworthy is that:

$$\forall\, 1 \le j \le n : \sum_{i=1}^{c} u_{i,j} = 1, \tag{4}$$

$$\forall\, 1 \le i \le c : \sum_{j=1}^{n} u_{i,j} > 0, \tag{5}$$

When the difference of $u_{i,j}$'s values in two consecutive calculation is less than a specific threshold, the calculation will stop.

Although the improvement can solve problems listed above, it consumes more time. Here, the improvements developed by Kolen et al. [41] and Yang et al. [42] were utilized. Kolen et al. [41] proposed to combine the update of centers of clusters and the membership matrix. Yang et al. [42] proposed to mark the cluster centers to distinguish them from sample points. These two methods were found to be useful to reduce the execution time.

This research refers to the land cover classification system from 2015, and images were first classified into eleven land use and land cover types and to identify potential classes. It is worth noting that some spectral classes correspond to various land use and land cover types with spectral similarities, for example grassland and farmland. Arguably, we followed previous studies [3,44,45], in which similar spectral were assigned to one land use and land cover type, which was of more importance for this research. Considering the local environment of the study area, the former eleven land use and land cover types were combined into three types: farmland, built land and water.

2.3.4. Accuracy Assessment

In total, 1000 random points were created using ArcGIS toolbox 10.2 (ESRI, Redlands, CA, USA) (Create Random Points) to evaluate the accuracy of both the classification results and the change detection results. Random points were created separately for each kind of classification result or change detection result, and the value of different results were masked into these points. The correctness of every point's value was evaluated manually.

This approach is divided into two main phases: the target area location phase and the target area-processing phase. This study used Landsat 8 OLI images whose spatial resolution is 30 m to execute the change detection.

3. Results

3.1. Assessment of the Improved/Standard Fuzzy c-Means Algorithm Based Classification

To evaluate the effectiveness of the improved fuzzy c-means in image classification, two kinds of fuzzy c-means algorithm were executed separately on image of study area of year 2015: one is the standard one, which uses the Euclidean distances to the cluster prototypes to calculate the membership degrees (the ED method); and the other is the improved one presented above, which use distances to the Voronoi cell of the cluster to calculate the membership degrees (the VD method) and made improvements to reduce the execution time. First, the images were classified to eleven land use and land cover types; second, the same types were merged; and, third, the image was classified into three types, built land, farmland and water (Figure 6). As stated in the Methodology, combining land use and land cover types may be imperfect, but it has been used in previous researches and also suitable for our research area. The results show that the VD methods produced more built land than ED methods. Three sites were selected randomly from the images, and the detailed comparison of these three sites confirmed that the VD methods identify much more built land than ED methods. To examine and quantify the accuracy of the classification algorithms, 1000 checkpoints (Figure 7) were created randomly using the toolbox in ArcGIS and the error matrixes were calculated utilizing these points (Tables 1 and 2).

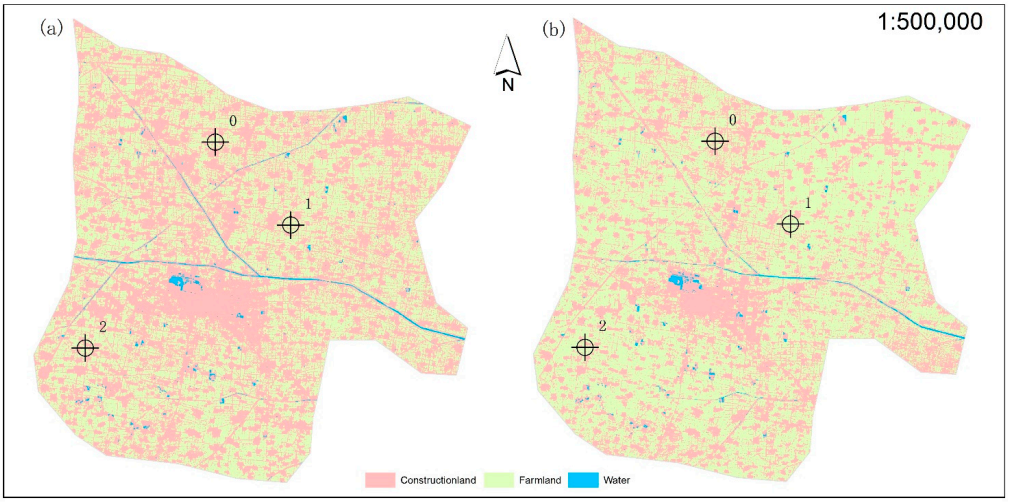

Figure 6. Classification results of land use and land cover types in Chengwu in year 2015: (**a**) the result of the improved FCM; and (**b**) the result of the standard FCM.

Table 1. The classification error matrix of VD (Voronoi Distance) method.

Land Cover Type	Built Land	Farmland	Water	Total	User's Accuracy (%)	Commission Error (%)
Built land	470	26	4	500	94.00	6.00
Farmland	13	387	0	400	96.75	3.25
Water	0	0	100	100	100.00	0.00
Total	483	413	104	1000		
Producer's Accuracy (%)	97.31	93.70	96.15			
Omission Error (%)	2.69	6.30	3.85			
Overall Accuracy (%)	95.70	Kappa Coefficient	0.93			

Figure 7. The 1000 checkpoints in Chengwu.

Table 2. The classification error matrix of ED (Euclidean Distance) method.

Land Cover Type	Built Land	Farmland	Water	Total	User's Accuracy (%)	Commission Error (%)
Built land	336	4	3	343	97.96	2.04
Farmland	149	408	0	557	73.25	26.75
Water	0	0	100	100	100.00	0.00
Total	485	412	103	1000		
Producer's Accuracy (%)	69.28	99.03	97.09			
Omission Error (%)	30.72	0.97	2.91			
Overall Accuracy (%)	84.40	Kappa Coefficient	0.74			

According to the error matrix, both the overall accuracy and the kappa coefficient of the VD method are better than those of the standard one. The biggest difference between these two methods was caused by the classification between built land and farmland. The classification results of the ED method show that there were many misclassifications between built land and farmland, i.e., much built land was classified as farmland. The user's and producer's accuracy also reflect that even the standard algorithm can correctly classify most of the farmland, but it also mistakenly classified some built land as farmland. The ED method's commission error of farmland and omission error of built land also reveal the same phenomenon.

The error matrix of VD matrix shows that both the omission error and commission error are small and the overall accuracy is high. It shows the capability of classifying pixels into the correct classes of this method is better than that of the standard one.

3.2. Assessment of Univariate Band/NDVI/Bi-Band Binary Masks Based Change Detection

The bi-band binary mask, NDVI binary mask and the univariate band binary mask were utilized to execute change detection on the study area.

The univariate band binary mask used the band 3 (0.53–0.59 μm) data for calculations and the result shows an area of 45.753 km^2 land with a likelihood of change (Figure 8a). The binary NDVI mask (Figure 8b) shows an area of 110.606 km^2 land that is suspected to have some changes in the land use and land cover types. The binary bi-band mask was derived from band 1 (0.43–0.45 μm) and band 5 (0.85–0.88 μm) according to the correlation coefficients of each pair of band (Table 3) from the

bi-temporal images. The result of binary bi-band mask (Figure 8c) shows that there are 165.834 km^2 area that is suspected to have changes. The area of target area of the univariate band binary mask varies greatly compared to the areas of the other two binary masks.

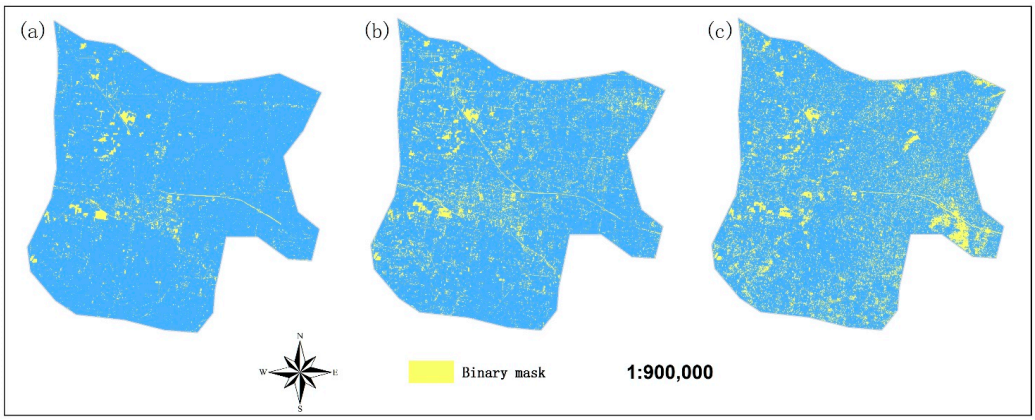

Figure 8. The binary masks: (**a**) band 3 binary mask; (**b**) NDVI binary mask; and (**c**) bi-band binary mask.

Table 3. Correlation coefficients of each pair of corresponding bands for the two temporal images.

Image 2015 \ Image 2013	Band 1	Band 2	Band 3	Band 4	Band 5	Band 6	Band 7
band 1	0.796						
band 2		0.814					
band 3			0.830				
band 4				0.848			
band 5					0.969		
band 6						0.882	
band 7							0.868

Through the information masked from the bi-temporal images by the binary masks, the change information was obtained utilizing the method presented before (Figure 9). The accuracy of those two methods is presented in Table 4.

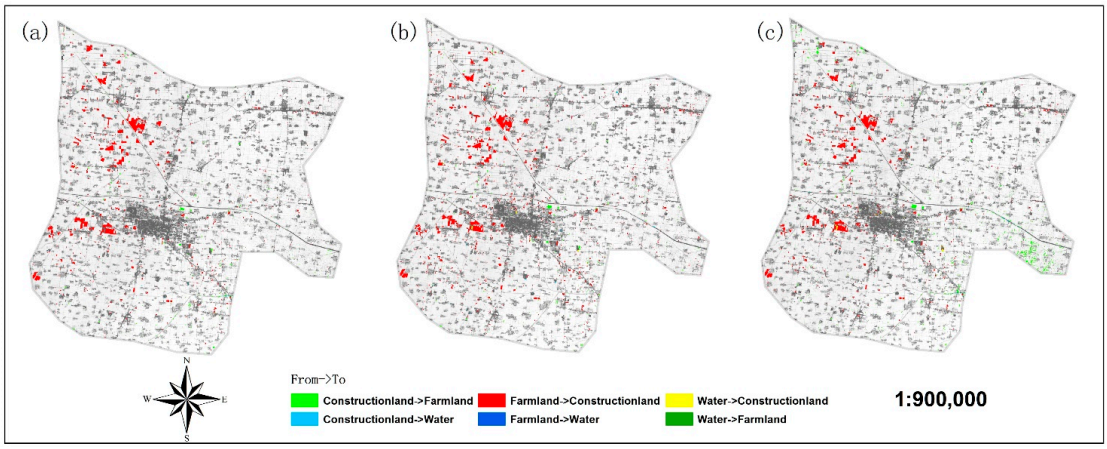

Figure 9. Change detection results: (**a**) the univariate band binary mask method; (**b**) the NDVI binary mask method; and (**c**) the bi-band binary mask method.

Table 4. The accuracy of the change detection result.

Land Cover Change Types $X \rightarrow Y$ [1]	Overall Accuracy (%)		
	Band 3 Mask	**NDVI Mask**	**Bi-Band Mask**
Built land → Farmland	85.71	100.00	100.00
Built land → Water	45.45	63.64	72.73
Farmland → Built land	88.24	88.68	94.12
Farmland → Water	50.00	66.67	66.67
Water → Built land	0.00	72.73	100.00
Water → Farmland	66.67	100.00	100.00
Average accuracy (%)	56.01	81.95	88.92

[1] $X \rightarrow Y$ means the land cover type changed from X to Y from 2013 to 2015.

The overall accuracy of the bi-band mask method (88.92%) is a little higher than that of the NDVI mask method (81.95%), and much higher than the univariate band binary mask's (56.01%).

The statistics information about the change detection results of these three methods in Table 5 shows that the three change detection results differs in some ways. The main changes are between built land and farmland, but the total areas are also different. The order of total area detected by the three methods is: NDVI > Bi-band > Univariate band.

Table 5. Comparison of change detection results of these three methods.

Land Cover Change Types	Area (km^2)		
	Band 3 Mask	**NDVI Mask**	**Bi-Band Mask**
Built land → Farmland	2.07	1.94	5.45
Built land → Water	0.11	0.23	0.11
Farmland → Built land	15.51	19.01	13.89
Farmland → Water	0.01	0.06	0.14
Water → Built land	0.00	0.16	0.28
Water → Farmland	0.06	0.00	0.08
Total area of detected	17.76	21.42	19.94
Built land Changed	13.33	17.00	8.60
Farmland Changed	−13.39	−17.12	−8.49
Water Changed	0.06	0.12	−0.12

By checking the results of these three methods, there are three sites where the largest differences were found between the univariate band mask and the bi-band mask (site 1, site 2 and site 3), and three sites with the largest differences between the NDVI mask and the bi-band mask (site 4, site 5 and site 6), as shown in Figure 10. Site 1, site 3, site 4 and site 6 illustrate change information detected by bi-band mask method and not detected by the univariate band mask or the NDVI mask method. Site 2 and site 5 illustrate the contrary situation, meaning detected by univariate band mask or NDVI mask method but not detected by bi-band mask method.

It can easily be found that the result of site 2 in univariate band mask, site 3 and site 6 in bi-band mask consistent with the field observation, and the other were false alarms. The result of site 1/site 4 was caused by the cloudlet contained in the image, which was only detected by the bi-band mask. The bi-band mask was influenced by cloudlet and regarded it as changed area, and the classification could not distinguish it from built land, resulting in the wrong detection. The result of site 5 was detected by the NDVI mask method only; the land cover type was changed from built land to farmland, and since NDVI is sensitive to plants change, it incorrectly regard it as changed area. The result of site 2 in the univariate band mask was true, while some of it was omitted in the bi-band mask.

Revising the wrong result in site 1 and site 2 in the bi-band mask change detection result, the change information of our study area is shown in Figure 11 and Table 6.

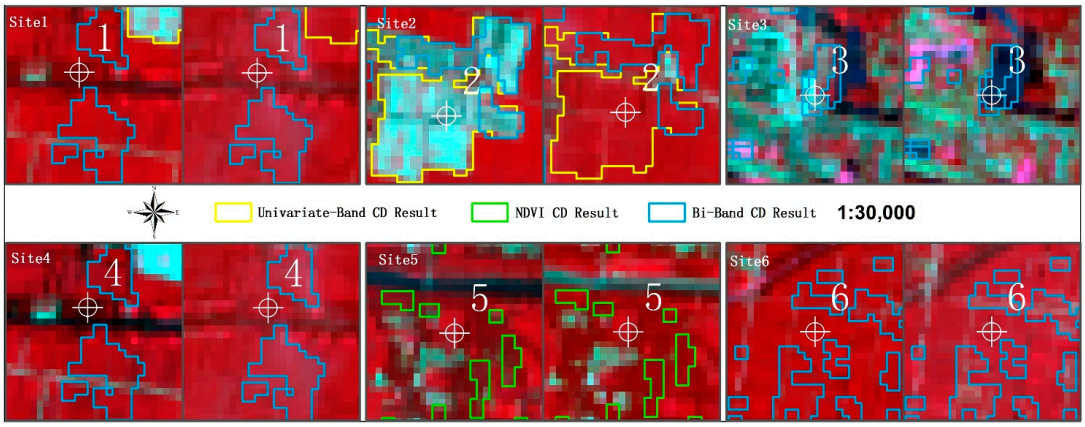

Figure 10. Sample sites for comparison of change detection between bi-band method and NDVI method (**left** picture for 2013, **right** picture for 2015).

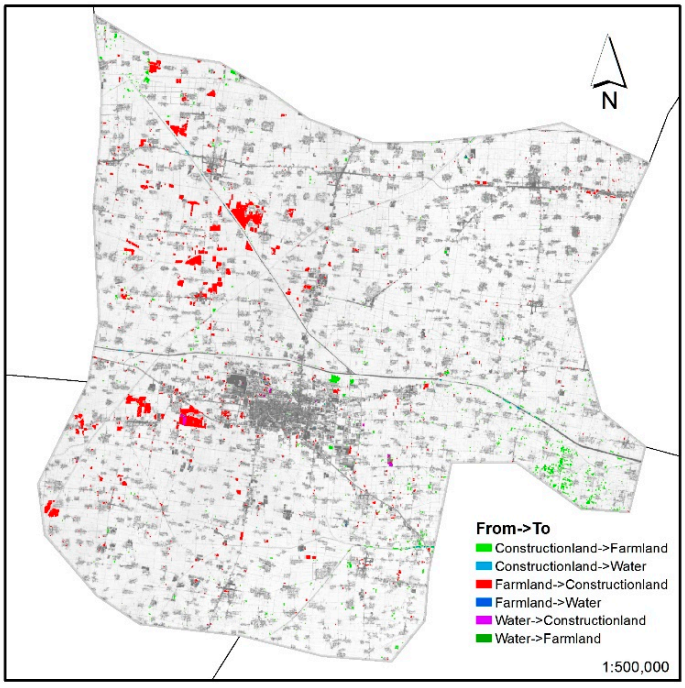

Figure 11. Change map of Chengwu from 2013 to 2015.

Table 6. The statistics of land cover change information extracted using bi-band mask.

Land Cover Change Types	Area (km^2)
Built land → Farmland	5.28
Built land → Water	0.11
Farmland → Built land	14.14
Farmland → Water	0.14
Water → Built land	0.28
Water → Farmland	0.08
Total area of detected	20.02
Built land Changed	9.03
Farmland Changed	−8.92
Water Changed	−0.12

The main changes of land cover happened between built land and farmland. Particularly, the change from farmland to built land is the largest one (14.14 km^2). Although part of the built land converted to farmland and water, the results manifest the increase of built land and the decrease of other land cover types in general. Totally, the area of built land increased by 9.03 km^2, farmland decreased by 8.92 km^2 and the water decreased by 0.12 km^2 during the research period. This urbanization process is similar to many cities in China [46–48].

4. Discussion

The change detection method proposed in this study proved to be effective, the accuracy of the change detection results of this method is high, and the workload was largely reduced by taking advantage of the binary mask; a more accurate information about the land cover/land use type was achieved using the improved fuzzy c-means algorithm

The overall accuracy of the bi-band binary mask is 88.92%, higher than that of the univariate band mask approach (56.01%) and the NDVI mask approach (81.95%). The overall accuracy and the kappa coefficient of the improved fuzzy c-means based classification (95.70%/0.93) are higher than those of the standard fuzzy c-means based one (84.40%/0.74). The improved one can distinguish built land and farmland well, while the standard one cannot. The producer's accuracy of the built land classified using the improved one is 97.31%, while that of the standard one is 69.28%. The user's accuracy of the farmland classified using the improved one is 96.75%, while that of the standard one is 73.25%.

With the help of the binary mask, many data were masked out, which largely reduced the amount of data needed to be processed. This binary mask approach can also apply on high resolution images that have a much more data to be processed, it would be helpful to reduce the workload and save the processing time.

Although the accuracy was improved, there are still some defects that need to be improved. (1) The improved fuzzy c-means algorithm proved useful in image classification and change detection in this study, and the accuracy of the classification results (Table 1) were better than the standard fuzzy c-means algorithm (Table 2). Nevertheless, it was only tested in our study area where the land cover type is simple; in other sites where the land cover type is complex, the classification effects of this algorithm need to be further tested. In addition, the accumulation error that would cause by the classification accuracy cannot be completely avoided. (2) Binary mask can help to reduce the data needed to be processed, but it can also bring some side effect such as ignoring neighborhood pixels, i.e., the neighborhood information of some pixels is unused, and this can probably cause some mistakes in the classification phase. (3) In this study, the threshold of bi-band difference image, univariate band difference image and the NDVI difference image were determined by trial and error, which greatly hindered the automation of this change detection method. (4) In our study area, it appears that the bi-band binary mask method cannot completely reduce the influence of the cloudlet, so care should be taken for the authenticity of the change detection result if one or both of the images contain cloud. (5) Similar to some other change detection methods, this approach was also affected by the variance in phenology [21,37,49]. The bi-band mask, NDVI mask or univariate band mask all require the phenology variance between the two periods to be smallest, otherwise it would be hard for this approach to handle the change detection.

Selecting the threshold through trial and error greatly hindered the automation. Singh [24] mentioned that the selection of the best threshold level should usually be associated with a prior knowledge about the scene or visual interpretation. Although it is difficult to select an appropriate threshold automatically, we will try to find an automatic way to solve this problem in the future work. The overall accuracy was high, but there are still shortages, such as the omission of some changed areas, which should be further studied to improve the performance in the future work. The accumulation error is inevitable; what we can do here is choose the classification method that can get the more accurate classification results.

5. Conclusions

The developed approach is divided into two phases: the target area location phase and the target area-processing phase. The bi-band binary mask was used to locate the suspected changed area to be our target area, reducing the amount of processing data and execution time, especially in the pixel-based unsupervised classification algorithm. The improved fuzzy c-means algorithm provided more accurate classification results. This study used Landsat 8 OLI images with spatial resolution of 30 m to execute the change detection. The change detection approach can not only help us locate the suspected changed area, but also get the detailed change information. The bi-band mask technique not only reduces the workload, but also provides as much information as possible about the changed area. The improved fuzzy c-means algorithm based unsupervised classification can avoid the manual intervention and decrease the influence of the subjective factor of researchers and it is less sensitive to noise, more time-saving, and the overall accuracy is high.

The combination of bi-band binary mask and fuzzy c-means algorithm for land-use change detection method was applied in Chengwu County, north China. The classification accuracy of this improved fuzzy c-means algorithm (95.70%) is better than that of the standard one (84.40%). In conclusion, the experimental results obtained on the bi-temporal remote sensing images demonstrate the effectiveness of the proposed method, and it could be applied in regional change detection.

Acknowledgments: This study was supported by the Natural Science Foundation of China (No. 41671429) and the Priority Academic Program Development of Jiangsu Higher Education Institutions (PAPD). The authors would like to thank the U.S. Geological Survey (http://glovis.usgs.gov/) for providing Landsat 8 OLI data.

Author Contributions: Xian Li and Shuhe Zhao conceived and designed the idea. Xian Li, Dianmin Cong and Zhaohua Zhang performed the experiments and analyzed the data. Xian Li, Shuhe Zhao and Hong Yang wrote the paper.

Conflicts of Interest: The authors declare no conflict of interest.

References

1. Houghton, R.A.; Hackler, J.L.; Lawrence, K.T. The U.S. Carbon Budget: Contributions from Land-Use Change. *Science* **1999**, *285*, 574. [CrossRef] [PubMed]
2. Jin, S.; Yang, L.; Danielson, P.; Homer, C.; Fry, J.; Xian, G. A comprehensive change detection method for updating the National Land Cover Database to circa 2011. *Remote Sens. Environ.* **2013**, *132*, 159–175. [CrossRef]
3. Peng, G.; Marceau, D.J.; Howarth, P.J. A comparison of spatial feature extraction algorithms for land-use classification with SPOT HRV data. *Remote Sens. Environ.* **1992**, *40*, 137–151.
4. Liu, Y.; Huang, X.; Yang, H.; Zhong, T. Environmental effects of land-use/cover change caused by urbanization and policies in Southwest China Karst area—A case study of Guiyang. *Habitat Int.* **2014**, *44*, 339–348. [CrossRef]
5. Zhang, M.; Huang, X.; Chuai, X.; Yang, H.; Lai, L.; Tan, J. Impact of land use type conversion on carbon storage in terrestrial ecosystems of China: A spatial-temporal perspective. *Sci. Rep.* **2015**, *5*, 10233. [CrossRef] [PubMed]
6. Lai, L.; Huang, X.; Yang, H.; Chuai, X.; Zhang, M.; Zhong, T.; Chen, Z.; Chen, Y.; Wang, X.; Thompson, J.R. Carbon emissions from land-use change and management in China between 1990 and 2010. *Sci. Adv.* **2016**, *2*, e1601063. [CrossRef] [PubMed]
7. Usman, M.; Liedl, R.; Shahid, M.A.; Abbas, A. Land use/land cover classification and its change detection using multi-temporal MODIS NDVI data. *J. Geogr. Sci.* **2015**, *25*, 1479–1506. [CrossRef]
8. Xian, G.; Homer, C.; Fry, J. Updating the 2001 National Land Cover Database land cover classification to 2006 by using Landsat imagery change detection methods. *Remote Sens. Environ.* **2009**, *113*, 1133–1147. [CrossRef]
9. Wang, A.S.; He, L. Practical split-window algorithm for retrieving land surface temperature over agricultural areas from ASTER data. *J. Appl. Remote Sens.* **2014**, *8*, 5230–5237. [CrossRef]
10. Ward, M.H.; Nuckols, J.R.; Weigel, S.J.; Maxwell, S.K.; Cantor, K.P.; Miller, R.S. Identifying populations potentially exposed to agricultural pesticides using remote sensing and a Geographic Information System. *Environ. Health Perspect.* **2000**, *108*, 5–12. [CrossRef] [PubMed]

11. Jat, M.K.; Garg, P.K.; Khare, D. Monitoring and modelling of urban sprawl using remote sensing and GIS techniques. *Int. J. Appl. Earth Observ. Geoinf.* **2008**, *10*, 26–43. [CrossRef]
12. Rahman, A.; Aggarwal, S.P.; Netzband, M.; Fazal, S. Monitoring Urban Sprawl Using Remote Sensing and GIS Techniques of a Fast Growing Urban Centre, India. *IEEE J. Sel. Top. Appl. Earth Observ. Remote Sens.* **2011**, *4*, 56–64. [CrossRef]
13. Hame, T.; Heiler, I.; San Miguel, J. An unsupervised change detection and recognition system for forestry. *Int. J. Remote Sens.* **1998**, *19*, 1079–1099. [CrossRef]
14. Quegan, S.; Toan, T.L.; Yu, J.J.; Ribbes, F.; Floury, N. Multitemporal ERS SAR analysis applied to forest mapping. *IEEE Trans. Geosci. Remote Sens.* **2000**, *38*, 741–753. [CrossRef]
15. Arieira, J.; Karssenberg, D.; Jong, S.M.D.; Addink, E.A.; Couto, E.G.; Cunha, C.N.D.; Ien, J.O.S. Integrating field sampling, geostatistics and remote sensing to map wetland vegetation in the Pantanal, Brazil. *Biogeosciences* **2011**, *8*, 667–686. [CrossRef]
16. Schmid, T.; Koch, M.; Gumuzzio, J. Multisensor approach to determine changes of wetland characteristics in semiarid environments (central Spain). *IEEE Trans. Geosci. Remote Sens.* **2005**, *43*, 2516–2525. [CrossRef]
17. Gitelson, A.; Garbuzov, G.; Szilagyi, F.; Mittenzwey, K.; Karnieli, A.; Kaiser, A. Quantitative remote sensing methods for real-time monitoring of inland waters quality. *Int. J. Remote Sens.* **2007**, *14*, 1269–1295. [CrossRef]
18. Sawaya, K.E.; Olmanson, L.G.; Heinert, N.J.; Brezonik, P.L.; Bauer, M.E. Extending satellite remote sensing to local scales: Land and water resource monitoring using high-resolution imagery. *Remote Sens. Environ.* **2003**, *88*, 144–156. [CrossRef]
19. Grover, K.; Quegan, S.; Costa Freitas, C.D. Quantitative estimation of tropical forest cover by SAR. *IEEE Trans. Geosci. Remote Sens.* **1999**, *37*, 479–490. [CrossRef]
20. Shixin, W.; Yi, Z.; Chengjie, W.; Yun, S.; Fuli, Y. Risk Evaluation on the Secondary Disasters of Dammed Lakes using Remote Sensing Datasets, in the "Wenchuan Earthquake". *J. Remote Sens.* **2008**, *12*, 900–907.
21. Kennedy, R.E.; Townsend, P.A.; Gross, J.E.; Cohen, W.B.; Bolstad, P.; Wang, Y.Q.; Adams, P. Remote sensing change detection tools for natural resource managers: Understanding concepts and tradeoffs in the design of landscape monitoring projects. *Remote Sens. Environ.* **2009**, *113*, 1382–1396. [CrossRef]
22. Hussain, M.; Chen, D.; Cheng, A.; Wei, H.; Stanley, D. Change detection from remotely sensed images: From pixel-based to object-based approaches. *ISPRS J. Photogramm. Remote Sens.* **2013**, *80*, 91–106. [CrossRef]
23. Fan, Y. Studies on Change Detection Methods for Multitemporal Remote Sensing. Master's Thesis, Xidian University, Xi'an, China, 2010.
24. Singh, A. Review Article Digital change detection techniques using remotely-sensed data. *Int. J. Remote Sens.* **1989**, *10*, 989–1003. [CrossRef]
25. Lu, D.; Mausel, P.; Brondízio, E.; Moran, E. Change detection techniques. *Int. J. Remote Sens.* **2004**, *25*, 2365–2401. [CrossRef]
26. Bovolo, F.; Camps-Valls, G.; Bruzzone, L. A support vector domain method for change detection in multitemporal images. *Pattern Recognit. Lett.* **2010**, *31*, 1148–1154. [CrossRef]
27. Ghosh, A.; Mishra, N.S.; Ghosh, S. Fuzzy clustering algorithms for unsupervised change detection in remote sensing images. *Inf. Sci.* **2011**, *181*, 699–715. [CrossRef]
28. Ghosh, S.; Mishra, N.S.; Ghosh, A. Unsupervised Change Detection of Remotely Sensed Images Using Fuzzy Clustering. In Proceedings of the International Conference on Advances in Pattern Recognition, Kolkata, India, 4–6 February 2009; pp. 385–388.
29. Mishra, N.S.; Ghosh, S.; Ghosh, A. Fuzzy clustering algorithms incorporating local information for change detection in remotely sensed images. *Appl. Soft Comput.* **2012**, *12*, 2683–2692. [CrossRef]
30. Zanotta, D.C.; Haertel, V.; Zanotta, D.C.; Haertel, V. Gradual land cover change detection based on multitemporal fraction images. *Pattern Recognit.* **2012**, *45*, 2927–2937. [CrossRef]
31. Chen, Y.; Cao, Z. An improved MRF-based change detection approach for multitemporal remote sensing imagery. *Signal Process.* **2013**, *93*, 163–175. [CrossRef]
32. Coppin, P.R.; Bauer, M.E. Processing of multitemporal Landsat TM imagery to optimize extraction of forest cover change features. *IEEE Trans. Geosci. Remote Sens.* **1994**, *32*, 918–927. [CrossRef]
33. Sanghamitra, B.; Sriparna, S. *Unsupervised Classification: Similarity Measures, Classical and Metaheuristic Approaches, and Applications*; Springer: New York, NY, USA, 2007; pp. 89–125.
34. Shalaby, A.; Tateishi, R. Remote sensing and GIS for mapping and monitoring land cover and land-use changes in the Northwestern coastal zone of Egypt. *Appl. Geogr.* **2007**, *27*, 28–41. [CrossRef]

35. Butt, A.; Shabbir, R.; Ahmad, S.S.; Aziz, N.; Nawaz, M.; Shah, M.T.A. Land cover classification and change detection analysis of rawal watershed using remote sensing data. *J. Biodivers. Environ. Sci.* **2015**, *6*, 2222–3045.
36. El-Kawy, O.R.A.; Rød, J.K.; Ismail, H.A.; Suliman, A.S. Land use and land cover change detection in the western Nile delta of Egypt using remote sensing data. *Appl. Geogr.* **2011**, *31*, 483–494. [CrossRef]
37. Munyati, C. Wetland change detection on the Kafue Flats, Zambia, by classification of a multitemporal remote sensing image dataset. *Int. J. Remote Sens.* **2000**, *21*, 1787–1806. [CrossRef]
38. Im, J.; Jensen, J.R.; Tullis, J.A. Object-based change detection using correlation image analysis and image segmentation. *Int. J. Remote Sens.* **2008**, *29*, 399–423. [CrossRef]
39. Fan, H.S.; Ai_Nai, M.A.; Jing, L.I. Case Study on Image Differencing Method for Land Use Change Detection Using Thematic Data in Renhe District of Panzhihua. *J. Remote Sens.* **2001**, *1*, 75–80. (In Chinese)
40. Hoppner, F.; Klawonn, F. A New apProach to Fuzzy Partitioning. In Proceedings of the Ifsa World Congress and Nafips International Conference, Vancouver, BC, Canada, 25–28 July 2001; Volume 3, pp. 1419–1424.
41. Kolen, J.F.; Hutcheson, T. Reducing the time complexity of the fuzzy c-means algorithm. *IEEE Trans. Fuzzy Syst.* **2002**, *10*, 263–267. [CrossRef]
42. Yang, S.; Min, L.I.; Peng, Z.G.; Feng, C. A Novel Multi-band Remote Sensing Image Change Detection Algorithm. *J. Image Graph.* **2009**, *14*, 572–578.
43. Zhu, L.; Chung, F.L.; Wang, S. Generalized fuzzy C-means clustering algorithm with improved fuzzy partitions. *IEEE Trans. Syst. Man Cybern. Part B Cybern. A Publ. IEEE Syst. Man Cybern. Soc.* **2009**, *39*, 578–591.
44. Mas, J.F. Monitoring land-cover changes: A comparison of change detection techniques. *Int. J. Remote Sens.* **2010**, *20*, 139–152. [CrossRef]
45. Vegaaraya, M. Applications of Hyper-Spectral and Radar Remote Sensing Analysis: A Case Study of Forest Landscapes in Costa Rica. Ph.D. Thesis, Georg-August University of Göottingen, Göttingen, Germany, November 2012.
46. Bai, X.; Shi, P.; Liu, Y. Realizing China's Urban dream. *Nature* **2014**, *509*, 158–160. [CrossRef] [PubMed]
47. Yang, H. China must continue the momentum of green law. *Nature* **2014**, *509*, 535. [CrossRef] [PubMed]
48. Yang, H. China's soil plan needs strong support. *Nature* **2016**, *536*, 375. [CrossRef] [PubMed]
49. Kim, D.-H.; Narashiman, R.; Sexton, J.O.; Huang, C. Methodology to select phenologically suitable Landsat scenes for forest change detection. In Proceedings of the Geoscience and Remote Sensing Symposium (IGARSS), Vancouver, BC, Canada, 24–29 July 2011; pp. 2613–2616.